Inorganica Chimica Acta, *170* (1990) 213–223

Synthesis, Characterisation, Oxygenation and Carbonylation of Ruthenium(III) Schiff Base Complexes

M. M. TAQUI KHAN*, N. H. KHAN, R. I. KURESHY, A. B. BORICHA and Z. A. SHAIKH

Discipline of Coordination Chemistry and Homogeneous Catalysis, Central Salt & Marine Chemicals Research Institute, Bhavnagar 364 002 (India)

(Received July 5, 1989; revised October 26, 1989)

Abstract

Some ruthenium(III) Schiff base complexes of the type $[RuLXY]^n$ where L = Schiff base namely, bis(α-hydroxyacetophenone)-*o*-phenylenediimine (α-acetop.oph), bis(2-hydroxy-4-methoxyacetophenone)-*o*-phenylenediimine (4-MeOacetop.oph), bis(α-hydroxyacetophenone)ethylenediimine (α-acetop.en), bis(2-hydroxy-4-methoxyacetophenone)ethylenediimine (4-MeOacetop.en), bis(α-hydroxyacetophenone)propylenediimine (α-acetop.prop), bis(2-hydroxy-4-methoxyacetophenone)propylendiimine (4-MeOacetop.prop), bis(α-hydroxyacetophenone)diethylenetriimine (α-acetop.dien), bis(2-hydroxy-4-methoxyacetophenone)diethylenetriimine (4-MeOacetop.dien), $n = -1$ when $X = Y = Cl^-$, $n = 0$ when X = imidazole (Im), 2-methylimidazole (2-MeIm) and $Y = Cl^-$ were synthesised and characterised by physicochemical methods. The reversible binding of molecular oxygen as well as carbon monoxide was carried out in DMF. The complexes show discrimination against the binding of CO over molecular oxygen as evinced by the values of K_{O_2} and K_{CO} in the complexes. The thermodynamic parameters $\Delta H°$, $\Delta G°$, $\Delta S°$ for the carbonylation and oxygenation reactions at 10, 25 and 40 °C are evaluated.

Introduction

Much attention has been recently given to the reversible binding of molecular oxygen and carbon monoxide as model systems in hemoproteins [1, 2]. The complexes capable of exhibiting reversible binding of O_2 play an important role in transport and storage of molecular oxygen [3–7]. The reactions of ruthenium porphyrins with small molecules such as CO and O_2 have also been the subject matter of considerable interest [8–11].

The reversible binding of carbon monoxide [12a, 12b] and dioxygen by Cu(I) complexes has been reported [12b] while CuCl supported on active carbon is a reversible CO carrier in the solid state [13–15]. Relatively few studies have been conducted on the equilibrium studies of metal carbonyl complexes in solution.

Some transition metal ions with variable oxidation states such as Mn(II) [6, 16], Co(II) [7], Fe(II) [17], Cu(I) [18] and Ni(II) [19] form dioxygen complexes having a different geometry and coordination number. A variety of tetracoordinated Co(II) [20–22] Schiff base complexes in the presence of axial bases show affinity for dioxygen binding depending on the coordinating groups surrounding the metal ion. Except for Co(II) Schiff base complexes the reversible oxygen binding capacity at ambient conditions is almost non-existent for other metal ions [6, 7].

In view of our growing interest in oxygenation and carbonylation of ruthenium(III) complexes for new water soluble catalysts [23], we report in this paper the synthesis and characterisation of some Ru(III) Schiff base complexes derived from the condensation reaction of α-hydroxyacetophenone, 2-hydroxy-4-methoxyacetophenone and amines. The reversible binding of O_2 and CO by these complexes was carried out in order to assess the difference in the dioxygen and CO affinities of these complexes which change with the σ donor capacity of the ligand coordinated to the metal ion. The complexes show a greater affinity for O_2 than for CO; hence equilibrium constant for carbonylation K_{CO} < equilibrium constant for oxygenation K_{O_2}. Such discrimination plays an important role in preventing poisoning by CO in hemoproteins [24–27]. In hemoglobin the distal effect of histidine produced by the globin chain is a major factor in discrimination. In our complexes, it is believed that the effect may be partly due to the steric effect of ligated ketones. The binding of molecular oxygen to the Ru(III) center in the Schiff base complexes involves a formal oxidation of metal by one electron with a simultaneous reduction of the coordinated dioxygen to a superoxo species. This is evidenced by a linear correlation between K_{O_2} and the Ru(IV)/Ru(III) redox couple. The carbonyl complexes are

---

*Author to whom correspondence should be addressed.

0020-1693/90/$3.50

of Ru(III) as evidenced by magnetic susceptibility measurements and other supporting data. The stability of dioxygen and carbonyl complexes is greater for 2-hydroxy-4-methoxyacetophenone and α-hydroxyacetophenone for the equatorial ligands and for the axial ligands Im > 2-MeIm > Cl^-. The enthalpy of dioxygen complexes is more exothermic and entropy $\Delta S°$ is more negative than for carbonyl complexes.

Experimental

$RuCl_3 \cdot 3H_2O$ (Johnson and Mathey), α-hydroxyacetophenone, 2-hydroxy-4-methoxyacetophenone, ethylenediamine, diethylenetriamine, propylenediamine, imidazole, 2-methylimidazole (Fluka), *o*-phenylenediamine (Alpha) were recrystallised twice from benzene before use. The Schiff bases derived from α-hydroxyacetophenone, 2-hydroxy-4-methoxyacetophenone with ethylenediamine, *o*-phenylenediamine, propylenediamine, diethylenetriamine were prepared by known procedures [28]. All the complexes were prepared under an oxygen free atmosphere. The progress of the reaction were checked by TLC from time to time.

Preparation of Complexes

Bis(α-hydroxyacetophenone)-o-phenylenediiminatodichloro ruthenate(III) (1); Bis(2-hydroxy-4-methoxyacetophenone)-o-phenylenediiminatodichloro ruthenate(III) (2); Bis(α-hydroxyactophenone)ethylenediiminatodichloro ruthenate(III) (3); Bis(2-hydroxy-4-methoxyacetophenone)ethylenediiminatodichloro ruthenate(III) (4); Bis(α-hydroxyacetophenone)propylenediiminatodichloro ruthenate(III) (5); Bis(2-hydroxy-4-methoxyacetophenone)propylenediiminatodichloro ruthenate(III) (6)

Hot ethanolic solutions (1.0 mmol) of the above ligands were added to 1.0 mmol of $K_2[RuCl_5 \cdot H_2O]$ in a 1:1 M:L ratio. The reaction mixture was refluxed up to 10–15 h in an argon atmosphere. The completion of the reaction was checked on TLC. After that the solution was filtered in an argon atmosphere. The filtrate was concentrated to about 10 ml and the complexes were precipitated by diethyl ether or ethylacetate. The complexes were recrystallised in the same solvent. They were dried *in vacuo*. Yield 60%.

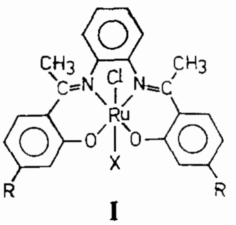

I

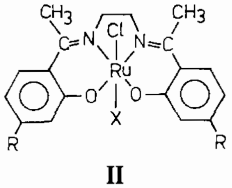

II

R=H, OCH3
X=Cl, Im, 2-Me Im

Bis(α-hydroxyacetophenone)-o-phenylenediiminatochloroimidazole ruthenium(III) (7); Bis(2-hydroxy-4-methoxyacetophenone)-o-phenylenediiminatochloroimidazole ruthenium(III) (8); Bis(α-hydroxyacetophenone)ethylenediiminatochloroimidazole ruthenium(III) (9); Bis(2-hydroxy-4-methoxyacetophenone)ethylenediiminatochloroimidazole ruthenium(III) (10); Bis(α-hydroxyacetophenone)propylenediiminatochloroimidazole ruthenium(III) (11); Bis(2-hydroxy-4-methoxyacetophenone)propylenediiminatochloroimidazole ruthenium(III) (12); Bis(α-hydroxyacetophenone)-o-phenylenediiminatochloro-2-methylimidazole ruthenium(III) (13); Bis(2-hydroxy-4-methoxyacetophenone)-o-phenylenediiminatochloro-2-methylimidazole ruthenium(III) (14); Bis(α-hydroxyacetophenone)-ethylenediiminatochloro-2-methylimidazole ruthenium(III) (15); Bis(2-hydroxy-4-methoxyacetophenone)ethylenediiminatochloro-2-methylimidazole ruthenium(III) (16); Bis(α-hydroxyacetophenone)propylenediiminatochloro-2-methylimidazole ruthenium(III) (17); Bis(2-hydroxy-4-methoxyacetophenone)propylenediiminatochloro-2-methylimidazole ruthenium(III) (18)

All these complexes were synthesised from their parent dichloro complexes [1–6]. After the completion of the synthesis of the dichloro complexes, the axial base ligand was added in a 1:1 molar ratio of axial base to the complexes. The reaction mixture was again refluxed for 8–10 h and the completion of the reaction checked on TLC. The compounds were isolated and recrystallised as described for the preparation of **1**–**6**. Yield 65%.

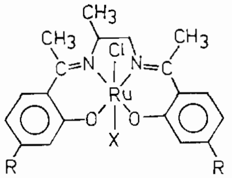

III

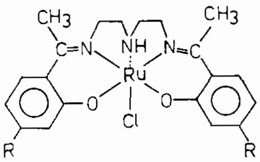

IV

R=H, OCH3
X=Cl, Im, 2-Me Im

Bis(α-hydroxyacetophenone)diethylenetriiminatochloro ruthenium(III) (19); Bis(2-hydroxy-4-methoxyacetophenone)diethylenetriiminatochloro ruthenium(III) (20)

The above mentioned ligands (1.0 mmol) were dissolved in ethanol and $K_2[RuCl_5 \cdot H_2O]$ (1.0 mmol) was mixed in a 1:1 M:L ratio. The reaction mixture was refluxed for 5–6 h in an argon atmosphere. After completion of the reaction the product was filtered, washed with ethanol and recrystallised in dry diethyl ether and ethylacetate. They were dried *in vacuo*. Yield 63%.

Physical Measurements

Microanalyses of the complexes were performed on a Carlo Erba Analyser model 1106. Molar conductance was measured at room temperature on a Digisun Electronics conductivity bridge. The IR spectra were recorded on a Nicolet 200 SXV FT-IR spectrometer in Nujol mulls/KBr. Electronic spectra were recorded on a Shimadzu UV–Vis recording spectrophotometer model 160. Cyclic voltammograms, d.c. Polarograms and differential pulse polarograms were recorded with a Princeton Applied Research (PAR) instrument as described earlier [29, 30]. The magnetic moment measurements were made at 298 K by the Gouy method using $Hg[Co(SCN)_4]$ as calibrant and experimental susceptibilities were corrected for diamagnetism.

Oxygen Uptake Measurements

The kinetics of oxygenation of all Schiff base complexes was investigated by the oxygen absorption technique in DMF at 10, 25 and 40 °C with the help of a manometric set up. The solubility of dioxygen was also measured separately in DMF at these three temperatures. The vapour pressure of the solvent was negligible over the temperature employed in this investigation. From the stoichometry of the reaction determined by dioxygen uptake and the corrected partial pressure of dioxygen at equilibrium, the oxygenation constant K_{O_2} as defined by eqn. (1) was calculated [31].

$$ML + O_2 \rightleftharpoons MLO_2 \qquad (1)$$

$$K_{O_2} = \frac{[MLO_2]}{[ML][O_2]}$$

The $P_{1/2}$ value (equilibrium O_2 pressure at half saturation) was calculated by the expression

$$P_{1/2} = \frac{K_h}{K_{O_2}}$$

where K_h = Henry's law constant given by the reciprocal of the solubility of O_2 in the medium at 1 atm. at a particular temperature. These constants are tabulated in Table 4).

CO Uptake Measurements

In order to calculate the equilibrium constant K_{CO} by UV–Vis spectrophotometry, solutions of the complexes were prepared in the concentration of 5×10^{-4} M in DMF saturated with CO by varying the concentration of CO in the range 1:1, 1:2 and 1:3 with respect to the degassed DMF. The spectrum was recorded immediately at 10, 25 and 40 °C by monitoring the peaks around (λ_{max} = 416–565 nm) and a constant value of absorbance was noted for each set. The solubility of carbon monoxide was also measured separately in DMF at different temperatures. The reaction of the complexes with CO may be written as

$$ML + CO \rightleftharpoons MLCO$$

$$K_{CO} = \frac{[MLCO]}{[ML][CO]}$$

The equilibrium constant K_{CO} was calculated by a reported method [32].

Results and Discussion

The stoichiometric composition of the complexes was consistent with the elemental analysis as given in Table 1. The complexes are high melting solids or decompose on melting. Millimolar solutions of complexes **1**–**6** in DMF are 1:1 electrolytes while the *trans* substituted imidazole or 2-methylimidazole complexes are non-electrolytes (Table 1). The magnetic moment μ_{eff} values in the range 1.97–2.08 BM confirm the complexes to be paramagnetic in nature (Table 1).

IR Spectra

A strong band at 3310 cm^{-1} in all the Schiff bases studied is assigned to ν(O–H). After complexation with the metal ion this band disappears showing the replacement of hydrogen by the metal atom. In such cases the ν(C–O) at 1280 cm^{-1} in the Schiff bases show a frequency shift towards lower frequency in the complexes [33]. An intense band in the range 1625–1635 cm^{-1} assigned to the azomethine group is red shifted on coordination to Ru(III). The ν(M–Cl) band is exhibited around 325 cm^{-1} in all the complexes (Table 2).

The UV–Vis spectral data are summarised in Table 2. In the UV region bands around 270 nm may be due to $\pi \rightarrow \pi^*$ transitions of the double bond of the azomethine group while a band near 350 nm is due to the $n\pi^*$ transition of non-bonding electrons present on the nitrogen of the azomethine group. After coordination with Ru(III) the bands show a hypsochromic shift (Table 2). A moderately intense band near 485 nm can be attributed to the charge transfer transition of the chloride ion [34]. All bands are undoubtedly charge transfer in origin except a band near 800 nm which can be assigned to a forbidden ligand field transition of Ru(III).

TABLE 1. Elemental analysis, molar conductance and magnetic moment of ruthenium(III) Schiff base complexes

Complex	Analysis: found (calc.) (%)				Molar conductance[a]	Magnetic moment μ_{eff}
	C	H	N	Cl		
K[Ru(α-acetop.oph)$\mathrm{Cl_2}$] (1)	47.57 (47.25)	3.62 (3.40)	5.04 (5.00)	12.78 (12.00)	75	1.98
K[Ru(4-MeO-acetop.oph)$\mathrm{Cl_2}$] (2)	46.98 (46.35)	3.61 (3.20)	4.56 (4.32)	11.57 (11.15)	90	1.97
K[Ru(α-acetop.en)$\mathrm{Cl_2}$) (3)	42.77 (42.25)	3.59 (3.00)	5.54 (5.25)	14.04 (13.75)	85	1.98
K[Ru(4-MeO-acetop.en)$\mathrm{Cl_2}$] (4)	42.48 (42.36)	3.92 (3.42)	4.95 (4.65)	12.55 (12.10)	80	1.98
K[Ru(α-acetop.prop)$\mathrm{Cl_2}$] (5)	43.76 (43.56)	4.25 (4.20)	5.37 (5.17)	13.61 (12.95)	95	1.97
K[Ru(4-MeO-acetop.prop)$\mathrm{Cl_2}$] (6)	43.52 (43.22)	4.17 (4.05)	4.83 (4.75)	12.25 (11.80)	70	1.97
[Ru(α-acetop.oph)ImCl] (7)	54.89 (54.65)	4.05 (3.95)	10.23 (10.00)	6.49 (6.00)	4	1.98
[Ru(4-MeO-acetop.oph)ImCl] (8)	52.56 (52.36)	4.24 (4.00)	9.42 (9.21)	5.97 (5.11)	5	1.98
[Ru(α-acetop.en)ImCl] (9)	50.55 (50.25)	4.44 (4.30)	11.22 (11.15)	7.11 (6.55)	5	1.98
[Ru(4-MeO-acetop.en)ImCl] (10)	49.41 (49.15)	4.68 (4.32)	10.01 (9.35)	6.35 (6.00)	3	1.97
[Ru(α-acetop.prop)ImCl] (11)	51.50 (51.32)	4.71 (4.25)	10.91 (9.65)	6.92 (5.89)	4	1.97
[Ru(4-MeO-acetop.prop)ImCl] (12)	50.30 (50.10)	4.92 (4.40)	9.77 (9.25)	6.19 (6.00)	6	1.97
[Ru(α-acetop.oph)2-MeImCl] (13)	55.66 (55.38)	4.31 (4.25)	9.98 (9.25)	6.32 (6.01)	2	1.98
[Ru(4-MeO-acetop.oph)2-MeImCl] (14)	54.14 (54.05)	4.54 (4.23)	9.01 (8.45)	4.21 (4.00)	3	1.98
[Ru(α-acetop.en)2-MeImCl] (15)	51.20 (51.00)	4.71 (4.25)	10.91 (10.25)	6.02 (6.09)	8	1.98
[Ru(4-MeO-acetop.en)2-MeImCl] (16)	49.24 (49.08)	5.03 (5.00)	9.98 (9.12)	6.32 (6.10)	4	1.98
[Ru(α-acetop.prop)2-MeImCl] (17)	52.41 (52.19)	4.97 (4.12)	10.62 (9.89)	6.73 (5.95)	5	1.98
[Ru(4-MeO-acetop.prop)2-MeImCl] (18)	51.14 (51.02)	5.15 (5.05)	9.53 (9.12)	6.04 (6.00)	4	1.98
[Ru(α-acetop.dien)Cl] (19)	50.68 (50.12)	4.89 (4.13)	8.86 (8.25)	7.49 (7.12)	4	2.08
[Ru(4-MeO-acetop.dien)Cl] (20)	49.48 (49.38)	5.09 (5.00)	7.86 (7.34)	6.64 (6.30)	3	2.08

[a] Molar conductivity at 298 K given in units of $\mathrm{ohm^{-1}\ cm^2\ m^{-1}}$; solvent is DMF.

On oxygenation, complexes **1**–**20** take up one mole of O_2 per mole of the complex which supports a 1:1 stoichiometry of metal ion to dioxygen in the complexes. The reaction with respect to molecular oxygen is reversible and coordinated dioxygen can be displaced from the metal centre by bubbling nitrogen through the solution. The reversible oxygenation reaction can therefore be written as

$$[\mathrm{Ru^{III}(L)(B)Cl}] + \mathrm{O_2} \overset{K_{\mathrm{O_2}}}{\rightleftharpoons} [\mathrm{Ru^{IV}(L)(B)(O_2{}^{-})}] + \mathrm{Cl^-}$$

TABLE 2. IR stretching frequency and UV–Vis data of ruthenium(III) Schiff base complexes

Complex	ν(C–O) (cm^{-1})	ν(C–N) (cm^{-1})	ν(M–Cl) (cm^{-1})	Imidazole peak (cm^{-1})	λ_{max} (ϵ (M^{-1} cm^{-2}))
K[Ru(α-acetop.oph)Cl_2] (1)	1265	1600	325		554(6000), 463(3405), 269(11355), 315(sh)(5665), 691(sh)(845)
K[Ru(4-MeO-acetop.oph)Cl_2] (2)	1270	1595	320		551(7565), 280(12500), 299(sh)(70690), 363(sh)(5165), 440(sh)(4690), 705(sh)(1200)
K[Ru(α-acetop.en)Cl_2] (3)	1250	1590	325		828(90), 452(2310), 346(2910), 264(3315)
K[Ru(4-MeO-acetop.en)Cl_2] (4)	1270	1595	320		793(70), 319(4960), 272(9320), 342(4200), 396(2395), 563(500)
K[Ru(α-acetop.prop)Cl_2] (5)	1255	1600	325		738(555), 588(1880), 409(2045), 326(9660), 268(10070)
K[Ru(4-MeO-acetop.prop)Cl_2] (6)	1260	1590	330		399(9480), 350(12495), 362(sh)(9580), 615(1450)
[Ru(α-acetop.oph)ImCl] (7)	1270	1600	320	98, 650, 1068	553(9530), 494(8890), 319(12495), 460(sh)(8410), 740(sh)(1050)
[Ru(4-MeO-acetop.oph)ImCl] (8)	1265	1610	325	615, 645, 1060	271(12060), 317(sh)(7745), 346(sh)(6110), 377(sh)(4765), 555(1060)
[Ru(α-acetop.en)ImCl] (9)	1250	1595	325	610, 640, 1060	450(1865), 348(2305), 264(2815)
[Ru(4-MeO-acetop.en)ImCl] (10)	1260	1600	320	615, 645, 1065	348(3130), 266(4380), 380(1990), 504(465)
[Ru(α-acetop.prop)ImCl] (11)	1270	1600	320	620, 655, 1065	746(120), 349(6045), 266(5285), 500(sh)(6400)
[Ru(4-MeO-acetop.prop)ImCl] (12)	1260	1595	325	625, 650, 1065	271(12060), 317(sh)(7745), 346(sh)(6110), 377(sh)(4765), 555(1060)
[Ru(α-acetop.oph)2-MeImCl] (13)	1265	1600	320	615, 670, 1130	565(10185), 280(12495), 350(sh)(6225), 460(sh)(6675), 495(sh)(7600), 532(sh)(9045), 743(1150)
[Ru(4-MeO-acetop.oph)2-MeImCl] (14)	1250	1610	324	620, 670, 1125	546(5525), 290(1250), 371(sh)(5280) 703(sh)(1550), 797(sh)(950)
[Ru(α-acetop.en)2-MeImCl] (15)	1265	1595	325	625, 670, 1120	348(3435), 265(4385), 407(sh)(2535) 512(770)
[Ru(4-MeO-acetop.en)2-MeImCl] (16)	1270	1600	330	620, 665, 1125	271(11400), 319(sh)(6800), 394(sh)(3640), 511(sh)(815)
[Ru(α-acetop.prop)2-MeImCl] (17)	1265	1598	325	620, 670, 1140	805(120), 348(6325), 266(5425), 356(sh)(5615), 410(sh)(2720)
[Ru(4-MeO-acetop.prop)2-MeImCl] (18)	1260	1590	320	620, 630, 1130	349(4375), 269(7680), 530(sh)(515), 402(sh)(2385), 314(sh)(4210)
[Ru(α-acetop.dien)Cl] (19)	1265	1610	325		450(1250), 325(1605), 264(2385)
[Ru(4-MeO-acetop.dien)Cl] (20)	1255	1600	320		308(8660), 270(12410), 379(sh)(2070), 525(sh)(720)

Oxygenation of the complexes results in the reversible oxidation of Ru(III) to a formal Ru(IV) oxidation state with the reduction of O_2 to unstable superoxide in O_2^-. The formation of Ru(IV) in the oxygenation solution was confirmed by electrochemical studies (Table 3). The cyclic voltammetry, d.c. polarograms and differential pulse polarograms of the complexes were recorded in nitrogen as well as in an oxygen atmosphere. The Ru(III)/Ru(II) couple observed in the presence of nitrogen lies in the range −0.525 to −0.616 V versus Ag/AgCl for all the complexes (Figs. 1(a) and 2(a)). However, when the same solutions were flushed with O_2, two waves appeared (Figs. 1(b) and 2(b)), one in

TABLE 3. Polarographic data for ruthenium(III) Schiff base complexes in DMF ($-E_{1/2}$ vs. Ag/AgCl)

Complex	Fresh solution under N_2	Oxygenated solution under O_2^-	
	Ru(III)/(II)	Ru(IV)/(III)O_2^-	Ru(III)/(II)O_2^-
K[Ru(α-acetop.oph)Cl_2] (1)	−0.598	−0.388	−0.728
K[Ru(4-MeO-acetop.oph)Cl_2] (2)	−0.601	−0.390	−0.730
K[Ru(α-acetop.en)Cl_2] (3)	−0.525	−0.325	−0.605
K[Ru(4-MeO-acetop.en)Cl_2] (4)	−0.530	−0.330	−0.620
K[Ru(α-acetop.prop)Cl_2] (5)	−0.552	−0.342	−0.673
K[Ru(4-MeO-acetop.prop)Cl_2] (6)	−0.560	−0.350	−0.680
[Ru(α-acetop.oph)ImCl] (7)	−0.614	−0.406	−0.759
[Ru(4-MeO-acetop.oph)ImCl] (8)	−0.616	−0.410	−0.761
[Ru(α-acetop.en)ImCl] (9)	−0.545	−0.327	−0.658
[Ru(4-MeO-acetop.en)ImCl] (10)	−0.548	−0.331	−0.662
[Ru(α-acetop.prop)ImCl] (11)	−0.592	−0.378	−0.712
[Ru(4-MeO-acetop.prop)ImCl] (12)	−0.595	−0.380	−0.720
[Ru(α-acetop.oph)2-MeImCl] (13)	−0.606	−0.399	−0.739
[Ru(4-MeO-acetop.oph)2-MeImCl] (14)	−0.610	−0.401	−0.749
[Ru(α-acetop.en)2-MeImCl] (15)	−0.538	−0.312	−0.648
[Ru(4-MeO-acetop.en)2-MeImCl] (16)	−0.541	−0.320	−0.656
[Ru(α-acetop.prop)2-MeImCl] (17)	−0.580	−0.355	−0.688
[Ru(4-MeO-acetop.prop)2-MeImCl] (18)	−0.582	−0.360	−0.700
[Ru(α-acetop.dien)Cl] (19)	−0.534	−0.310	−0.646
[Ru(4-MeO-acetop.dien)Cl] (20)	−0.537	−0.311	−0.647

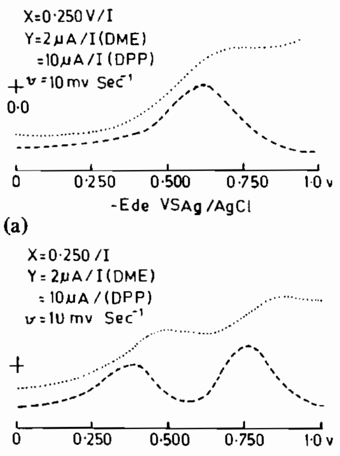

Fig. 1. Polarogram and differential pulse polarogram of K[Ru(α-acetop.oph)Cl_2] (1 mM) solution at 25 °C in DMF solvent using tetrabutylammoniumperchlorate as supporting electrolyte: (a) under nitrogen; (b) under oxygen.

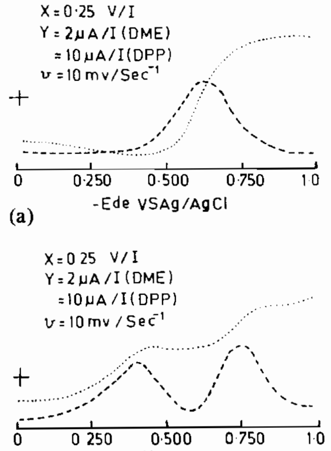

Fig. 2. Polarogram and differential pulse polarogram of K[Ru(4-MeO-acetop.oph)Cl_2] (1 mM) solution at 25 °C in DMF solvent using tetrabutylammoniumperchlorate as supporting electrolyte: (a) under nitrogen; (b) under oxygen.

the range −0.310 to −0.342 which is due to the Ru(IV)/Ru(III) couple while the other wave at −0.605 to −0.761 is assigned to the reduction of dissolved [35] molecular oxygen ($O_2 + e^- \rightarrow O_2^-$). The Ru(III)/Ru(II) couple is masked by the O_2/O_2^- reduction. By flushing nitrogen through the oxygenated solutions, both the redox peaks corresponding to Ru(IV)/Ru(III) and O_2/O_2^- disappear with the appearance of the Ru(III)/Ru(II) redox couple at the same potentials as was observed for the original Ru(III) complexes under nitrogen atmosphere. This observation supports the reversible binding of molecular oxygen to the Ru(III) complexes.

The electronic spectra of the oxygenated species were scanned in DMF and do not show any remarkable change as a consequence of oxygenation and

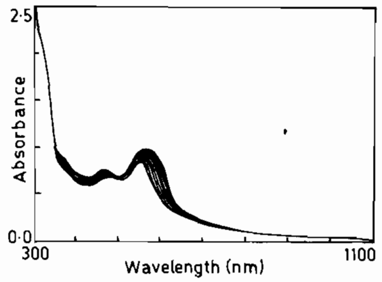

Fig. 3. The UV–Vis absorption spectral changes during carbonylation of [Ru(α-acetop.oph)ImCl] in DMF (1 × 10^{-3} M) with time: ——, soon after preparation; – – –, after 4 h; in 15 min intervals at 303 K and path length l = 0.2 cm.

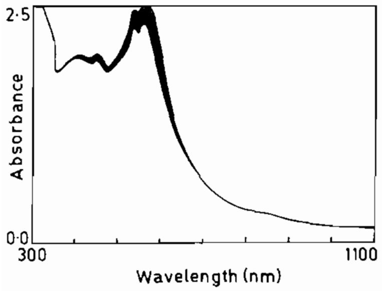

Fig. 4. The UV–Vis absorption spectral change during carbonylation of [Ru(4-MeO-acetop.oph)ImCl] in DMF (1 × 10^{-3} M) with time: ——, soon after preparation; – – –, after 4 h; in 15 min intervals at 303 K and path length l = 0.2 cm.

only a modest increase in absorbance was observed. This behaviour was also reported by Chen and Martell [31].

In order to evaluate the equilibrium constant for carbonylation, the UV–Vis spectra of the complexes were recorded in DMF saturated with CO by varying the concentration of CO in the ratio 1:1, 1:2 and 1:3 with respect to degassed DMF. In all the complexes, there is an increase in absorbance in the range λ_{max} = 416–565 nm with time. Electronic spectra of [Ru(α-acetop.oph)ImCl] and [Ru(4-MeO-acetop.oph)ImCl] in DMF saturated with CO are depicted in Figs. 3 and 4. A maximum increase is observed at 561 and 454 nm in both cases and is assigned to the MLCT band. Carbonylation of the complexes does not cause a reduction of Ru(III) to Ru(II). This was confirmed by the observation of the Ru(III)/Ru(II) couple in d.c. and differential pulse polarograms of the solutions at −0.301 to −0.505 V of these complexes saturated with CO gas. The Ru(II)/Ru(I) peak was absent in the DPP of the couples. The reversible binding of CO is confirmed by flushing N_2 through the solution which displaces CO. This reflects on the low stability of the Ru(III) carbonyl complexes over those of the Ru(II) carbonyl species which are more stable because of the greater softness and lower value of electronegativity of Ru(II) as compared to Ru(III). The equilibrium constants for oxygenation, K_{O_2} and carbonylation, K_{CO} (Tables 4 and 5) depend on the nature of the axial ligand and decrease in the order Im > 2-MeIM > Cl. This is due to the greater σ donor capacities of imidazole and 2-methylimidazole as compared to chloro causing an increase in electron density at the metal centre which in turn increases the dπ–pπ back donation from the metal ion to the coordinated CO, thereby, increasing the stability of the corresponding complexes. However, the O_2 stability increases because of a better energy match

TABLE 4. Thermodynamic constants for dioxygen binding to ruthenium(III) Schiff base complexes in DMF at 1 atmosphere

Complex	Temperature (°C)	log K_{O_2}	$P_{1/2}$ (torr)	$\Delta H°$ (K cal/mol)	$\Delta G°$ (K cal/mol)	$\Delta S°$ (e.u.)
K[Ru(α-acetop.oph)Cl_2) (1)	10	3.16 ± 0.01	0.118 ± 0.001			
	25	2.57 ± 0.1	0.504 ± 0.014	−13.8 ± 0.5	−3.50 ± 0.01	−35 ± 1
	40	2.13 ± 0.01	1.62 ± 0.400			
K[Ru(4-MeO-acetop.oph)Cl_2] (2)	10	3.33 ± 0.01	0.078 ± 0.002			
	25	2.71 ± 0.006	0.365 ± 0.004	−15.5 ± 0.3	−3.7 ± 0.01	−39 ± 1
	40	2.18 ± 0.01	1.43 ± 0.010			
K[Ru(α-acetop.en)Cl_2] (3)	10	2.80 ± 0.01	0.265 ± 0.002			
	25	2.45 ± 0.01	0.664 ± 0.010	−11.0 ± 0.6	−3.34 ± 0.01	−28 ± 1
	40	1.98 ± 0.01	2.27 ± 0.050			
K[Ru(4-MeO-acetop.en)Cl_2] (4)	10	2.95 ± 0.01	0.189 ± 0.003			
	25	2.51 ± 0.01	0.579 ± 0.008	−12.3 ± 0.4	−3.42 ± 0.1	−30 ± 2
	40	2.04 ± 0.01	2.00 ± 0.004			
K[Ru(α-acetop.prop)Cl_2] (5)	10	3.01 ± 0.01	0.164 ± 0.002			
	25	2.53 ± 0.01	0.550 ± 0.008	−13.0 ± 0.2	−3.45 ± 0.01	−32 ± 1
	40	2.04 ± 0.01	1.96 ± 0.010			

(continued)

TABLE 4. *(continued)*

Complex	Temperature (°C)	log K_{O_2}	$P_{1/2}$ (torr)	$\Delta H°$ (K cal/mol)	$\Delta G°$ (K cal/mol)	$\Delta S°$ (e.u.)
K[Ru(4-MeO-acetop.prop)Cl$_2$] (6)	10	3.24 ± 0.01	0.097 ± 0.003			
	25	2.67 ± 0.01	0.401 ± 0.007	−14.3 ± 0.2	−3.64 ± 0.01	−36 ± 1
	40	2.18 ± 0.01	1.44 ± 0.020			
[Ru(α-acetop.oph)ImCl] (7)	10	3.91 ± 0.01	0.021 ± 0.001			
	25	2.91 ± 0.01	0.229 ± 0.007	−21.0 ± 1	−3.9 ± 0.02	−60 ± 3
	40	2.29 ± 0.01	1.11 ± 0.003			
[Ru(4-MeO-acetop.oph)ImCl] (8)	10	3.94 ± 0.01	0.024 ± 0.005			
	25	2.98 ± 0.01	0.194 ± 0.006	−22.2 ± 0.7	−4.06 ± 0.02	−60 ± 2
	40	2.29 ± 0.01	1.11 ± 0.030			
[Ru(α-acetop.en)ImCl] (9)	10	3.23 ± 0.01	0.099 ± 0.003			
	25	2.69 ± 0.01	0.378 ± 0.007	−14.1 ± 0.2	−3.67 ± 0.02	−35 ± 1
	40	2.18 ± 0.01	1.44 ± 0.020			
[Ru(4-MeO-acetop.en)ImCl] (10)	10	3.48 ± 0.01	0.055 ± 0.001			
	25	2.71 ± 0.01	0.35 ± 0.010	−18 ± 0.5	−3.7 ± 0.01	−48 ± 1
	40	2.13 ± 0.01	1.54 ± 0.030			
[Ru(α-acetop.prop)ImCl] (11)	10	3.65 ± 0.01	0.037 ± 0.001			
	25	2.78 ± 0.01	0.309 ± 0.005	−19.0 ± 1	−3.79 ± 0.01	−49 ± 3
	40	2.24 ± 0.01	1.25 ± 0.020			
[Ru(4-MeO-acetop.prop)ImCl] (12)	10	3.68 ± 0.01	0.037 ± 0.001			
	25	2.87 ± 0.01	0.253 ± 0.005	−19.3 ± 0.30	−3.90 ± 0.02	−52 ± 1
	40	2.22 ± 0.01	1.31 ± 0.020			
[Ru(α-acetop.oph)2-MeImCl] (13)	10	3.46 ± 0.01	0.058 ± 0.002			
	25	2.71 ± 0.01	0.362 ± 0.005	−16.7 ± 0.60	−3.70 ± 0.01	−44 ± 2
	40	2.21 ± 0.01	1.31 ± 0.020			
[Ru(4-MeO-acetop.oph)2-MeImCl] (14)	10	3.65 ± 0.01	0.037 ± 0.001			
	25	2.77 ± 0.01	0.309 ± 0.010	−18.0 ± 1	−3.79 ± 0.01	49 ± 4
	40	2.28 ± 0.01	1.11 ± 0.030			
[Ru(α-acetop.en)2-MeImCl] (15)	10	3.08 ± 0.01	0.140 ± 0.004			
	25	2.54 ± 0.01	0.543 ± 0.009	−12.7 ± 0.40	−3.46 ± 0.01	31 ± 1
	40	2.14 ± 0.01	1.59 ± 0.030			
[Ru(4-MeO-acetop.en)2-MeImCl] (16)	10	3.16 ± 0.01	0.115 ± 0.003			
	25	2.61 ± 0.01	0.456 ± 0.006	−13.9 ± 0.20	−3.51 ± 0.50	35 ± 0.5
	40	2.13 ± 0.01	1.60 ± 0.030			
[Ru(α-acetop.prop)2-MeImCl] (17)	10	3.24 ± 0.01	0.097 ± 0.001			
	25	2.64 ± 0.01	0.427 ± 0.006	−14.6 ± 0.20	−3.60 ± 0.01	37 ± 1
	40	2.15 ± 0.01	1.53 ± 0.040			
[Ru(4-MeO-acetop.prop)2-MeImCl] (18)	10	2.33 ± 0.01	0.078 ± 0.002			
	25	2.71 ± 0.01	0.366 ± 0.005	−15.1 ± 0.2	−3.69 ± 0.01	38 ± 1
	40	2.21 ± 0.01	1.33 ± 0.020			
[Ru(α-acetop.dien)Cl] (19)	10	3.02 ± 0.01	1.60 ± 0.002			
	25	2.48 ± 0.01	0.624 ± 0.012	−13.5 ± 0.1	−3.38 ± 0.01	−34.0 ± 1
	40	2.01 ± 0.01	2.10 ± 0.020			
[Ru(4-MeO-acetop.dien)Cl] (20)	10	3.24 ± 0.01	0.096 ± 0.002			
	25	2.64 ± 0.01	0.427 ± 0.011	−14.8 ± 0.2	−3.60 ± 0.02	38 ± 1
	40	2.14 ± 0.01	1.57 ± 0.040			

TABLE 5. Thermodynamic constants for carbon monoxide binding to ruthenium(III) Schiff base complexes in DMF at 1 atmosphere

Complex	Temperature (°C)	log K_{CO}	$P_{1/2}$ (torr)	$\Delta H°$ (K cal/mol)	$\Delta G°$ (K cal/mol	$\Delta S°$ (e.u.)
[Ru(α-acetop.oph)Cl$_2$] (1)	10	2.11 ± 0.01	1.18 ± 0.020			
	25	1.93 ± 0.01	1.94 ± 0.060	−6.4 ± 0.1	−2.51 ± 0.02	−13 ± 0.4
	40	1.73 ± 0.01	3.50 ± 0.070			

(continued)

TABLE 5. *(continued)*

Complex	Temperature (°C)	$\log K_{CO}$	$P_{1/2}$ (torr)	ΔH° (K cal/mol)	ΔG° (K cal/mol)	ΔS° (e.u.)
K[Ru(4-MeO-acetop.oph)Cl_2] (2)	10	2.32 ± 0.01	0.714 ± 0.010			
	25	1.96 ± 0.01	1.83 ± 0.050	−7.7 ± 0.4	−2.67 ± 0.02	−17 ± 1
	40	1.75 ± 0.01	3.26 ± 0.040			
K[Ru(α-acetop.en)Cl_2]	10	2.00 ± 0.01	1.51 ± 0.020			
	25	1.79 ± 0.01	2.67 ± 0.040	−5.0 ± 0.1	−2.45 ± 0.01	−8.2 ± 0.2
	40	1.62 ± 0.01	4.39 ± 0.070			
K[Ru(4-MeO-acetop.en)Cl_2] (4)	10	2.11 ± 0.01	0.114 ± 0.002			
	25	1.89 ± 0.01	2.14 ± 0.020	−5.8 ± 0.1	−2.62 ± 0.01	−10 ± 0.3
	40	1.68 ± 0.01	3.80 ± 0.090			
K[Ru(α-acetop.prop)Cl_2] (5)	10	2.05 ± 0.01	1.33 ± 0.020			
	25	1.82 ± 0.01	2.49 ± 0.060	−5.4 ± 0.2	−2.49 ± 0.1	−10 ± 0.7
	40	1.70 ± 0.01	3.63 ± 0.70			
K[Ru(4-MeO-acetop.prop)Cl_2] (6)	10	2.29 ± 0.01	0.760 ± 0.014			
	25	1.96 ± 0.01	1.76 ± 0.010	−7.3 ± 0.4	−2.67 ± 0.02	−16 ± 1
	40	1.75 ± 0.01	3.27 ± 0.050			
[Ru(α-acetop.oph)ImCl] (7)	10	2.44 ± 0.01	0.543 ± 0.026			
	25	2.00 ± 0.01	1.69 ± 0.030	−8.3 ± 0.2	−2.71 ± 0.01	−19 ± 3
	40	1.82 ± 0.01	2.77 ± 0.070			
[Ru(4-MeO-acetop.oph)ImCl] (8)	10	2.48 ± 0.01	0.493 ± 0.008			
	25	2.06 ± 0.01	1.43 ± 0.040	−10.4 ± 0.1	−2.81 ± 0.01	−26 ± 1
	40	1.70 ± 0.01	3.63 ± 0.070			
[Ru(α-acetop.en)ImCl] (9)	10	2.05 ± 0.01	1.33 ± 0.020			
	25	1.82 ± 0.01	2.49 ± 0.060	−5.7 ± 0.10	−2.49 ± 0.1	−11 ± 1
	40	1.62 ± 0.01	4.40 ± 0.060			
[Ru(4-MeO-acetop.en)ImCl] (10)	10	2.23 ± 0.01	0.88 ± 0.009			
	25	1.98 ± 0.01	1.75 ± 0.030	−7.9 ± 0.5	−2.70 ± 0.01	−17 ± 2
	40	1.64 ± 0.01	4.25 ± 0.090			
[Ru(α-acetop.prop)ImCl] (11)	10	2.27 ± 0.01	0.809 ± 0.020			
	25	1.98 ± 0.01	1.72 ± 0.030	−8.4 ± 0.4	−2.70 ± 0.01	−19 ± 2
	40	1.64 ± 0.01	4.25 ± 0.090			
[Ru(4-MeO-acetop.prop)ImCl] (12)	10	2.40 ± 0.01	0.588 ± 0.100			
	25	2.11 ± 0.01	1.30 ± 0.030	−10.1 ± 0.7	−2.87 ± 0.01	−24 ± 2
	40	1.65 ± 0.01	4.25 ± 0.090			
[Ru(α-acetop.oph)2-MeImCl] (13)	10	2.22 ± 0.01	0.912 ± 0.012			
	25	2.00 ± 0.01	1.64 ± 0.020	−8.3 ± 1	−2.73 ± 0.01	−19 ± 3
	40	1.59 ± 0.01	4.79 ± 0.040			
[Ru(4-MeO-acetop.oph)2-MeImCl] (14)	10	2.45 ± 0.01	0.531 ± 0.010			
	25	2.07 ± 0.01	1.40 ± 0.040	−10.0 ± 0.2	−2.82 ± 0.01	−24 ± 1
	40	1.70 ± 0.01	3.63 ± 0.060			
[Ru(α-acetop.en)2-MeImCl] (15)	10	2.00 ± 0.01	1.50 ± 0.030			
	25	1.81 ± 0.06	2.60 ± 0.340	−5.1 ± 0.6	−2.40 ± 0.01	−9 ± 2
	40	1.62 ± 0.01	4.44 ± 0.040			
[Ru(4-MeO-acetop.en)2-MeImCl] (16)	10	2.20 ± 0.01	1.01 ± 0.050			
	25	1.86 ± 0.01	2.27 ± 0.050	−7.7 ± 0.2	−2.54 ± 0.01	−17 ± 1
	40	1.62 ± 0.01	4.40 ± 0.060			
[Ru(α-acetop.prop)2-MeImCl] (17)	10	2.12 ± 0.01	1.12 ± 0.010			
	25	1.81 ± 0.01	2.63 ± 0.070	−6.8 ± 0.4	−2.46 ± 0.01	−15 ± 1
	40	1.62 ± 0.01	4.46 ± 0.040			
[Ru(4-MeO-acetop.prop)2-MeImCl] (18)	10	2.34 ± 0.01	0.677 ± 0.011			
	25	2.04 ± 0.01	1.50 ± 0.030	−7.4 ± 0.1	−2.78 ± 0.01	−15 ± 1
	40	1.79 ± 0.01	2.96 ± 0.070			
[Ru(α-acetop.dien)2-MeImCl] (19)	10	2.32 ± 0.01	0.719 ± 0.016			
	25	2.06 ± 0.01	1.45 ± 0.030	−7.5 ± 0.3	−2.80 ± 0.02	−16 ± 1
	40	1.76 ± 0.01	3.20 ± 0.050			
[Ru(4-MeO-acetop.dien)2-MeImCl] (20)	10	2.39 ± 0.01	0.604 ± 0.013			
	25	2.00 ± 0.01	1.69 ± 0.060	−8.2 ± 0.6	−2.72 ± 0.01	−19 ± 2
	40	1.78 ± 0.01	3.02 ± 0.060			

between the O_2 π^* and metal d orbitals. In the case of 2-methylimidazole which is more basic than imidazole, the values of log K_{O_2} and K_{CO} are lower than those of the imidazole complexes. This may be due to the steric hinderance by the methyl group which predominates over the higher basicity of 2-methylimidazole [29]. The stability of dioxygen and carbonyl complexes with respect to equatorial ligands decreases in the order 4-MeO-acetop.oph > α-acetop.oph > 4-MeO-acetop.prop > α-acetop.prop > 4-MeO-acetop.dien > α-acetop.dien > 4-MeO-acetop.en > α-acetop.en.

The 4-MeO-acetop.oph complexes are more stable than 4-MeO-acetop.en complexes. The same trend was also observed [29] in bis(salicylaldehyde)-*o*-phenylenediimine (saloph) complexes which are more stable than bis(salicylaldehyde)ethylenediimine (salen) complexes. This seems to be a structural effect of the doming in the case of 4-MeO-acetop.oph, α-acetop.oph and saloph complexes which increases the stability of the dioxygen and carbonyl complexes. Doming of the equatorial ligand also plays an important role in the dioxygen affinity of porphyrins [24–26].

The stability of the carbonyl complexes of Ru(III) are about an order of magnitude lower than those of dioxygen complexes (Tables 4 and 5). The complexes, thus, exhibit discrimination towards CO binding. Though the electronic effects of the axial and equatorial ligands are about the same for the carbonyl and dioxygen complexes, the lower stability of the Ru(III) carbonyls seems to be due to a decrease in the dπ–pπ backbonding to CO in these complexes. The situation is, therefore, the reverse of the Fe(II) porphyrins [24, 25] where the CO exhibits a stronger bonding to the metal ion than dioxygen. The discrimination against CO binding in Fe(II) porphyrins comes mostly from the steric effects such as the interaction of distal histidine in hemoglobin or the size of the pocket [26] containing the CO or the O_2 group [26]. In the Ru(III) carbonyls studied, the CO is reversibly bonded and is displaced by bubbling N_2 through the solution in contrast to irreversible binding of CO in Fe(II) porphyrins [24, 25].

The values of thermodynamic parameters ΔG°, ΔH° and ΔS° associated with equilibrium constant for oxygenation K_{O_2} are in agreement with those reported earlier [29, 30, 36]. The enthalpies are highly exothermic and entropies are fairly negative. From Table 5 it is ascertained that ΔH° is greater for 4-MeOacetop.oph than for α-acetop.oph which reflects on the greater σ-donor capacity of the attached methoxy group causing the highest metal–oxygen bond strength in complexes of this series.

The carbonyl complexes also show the same trend for thermodynamic parameters ΔH°, ΔS° and ΔG°. The enthalpy values ΔH° for Ru(III) carbonyls is more positive than those of the dioxygen complexes which reflects on a weaker M–CO bond in carbonyls than the metal–dioxygen bond. The entropies are about -8.3 ± 0.2 e.u. to 24.2 ± 2.0 e.u. more positive than the dioxygen complexes showing a comparatively lower [29, 30] loss of vibrational and rational degree of freedom of CO on coordination as compared to O_2.

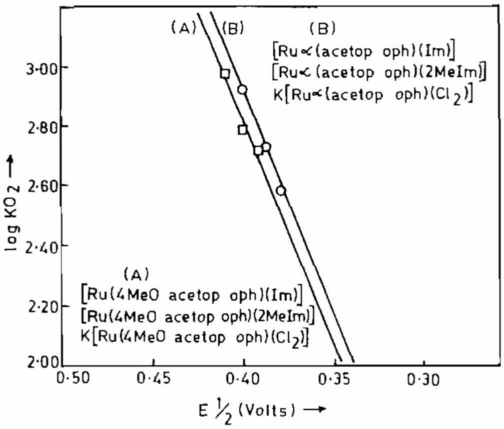

Fig. 5. Correlation of log K_{O_2} (25°) with Ru(IV)–Ru(III) peak potentials for superoxo complexes (A) 2, 7 and 14 and (B) 1, 7 and 13.

A good correlation has been found between the log K_{O_2} and $E_{1/2}$ values of Ru(IV)/Ru(III) couple in the dioxygen complexes as depicted in Fig. 5. This correlation reflects on the ease of oxidation of Ru(III) → Ru(IV) as the redox potential of Ru(IV)/Ru(III) couple is shifted to more negative values. This negative shift depends on an increase in charge density on the metal ion by the equatorial and axial ligands. In such cases, the transfer of electron density from metal to dioxygen becomes easier resulting in stabilisation of the dioxygen complexes and the coordination of a formal superoxide ion to a formal Ru(IV) ion. A similar trend was observed between the $E_{1/2}$ values of Co(III)/Co(II) couple and the log K_{O_2} values for a series of Co(II) Schiff base complexes [37].

References

1 J. P. Collman, T. R. Halbert and K. S. Suslick, in T. Spiro (ed.), *Metal Ion Activation of Dioxygen*, Wiley Interscience, New York, 1980, pp. 1–72.

2 C. K. Chang and T. G. Taylor, *J. Am. Chem. Soc.*, *95* (1973) 5810.

3 M. M. Taqui Khan and A. E. Martell, *Homogeneous Catalysis by Metal Complexes*, Vols. I and II, Academic Press, New York, 1974.

4 G. McLendon and A. E. Martell, *Coord. Chem. Rev., 19* (1976) 1.

5 J. P. Collman, *Acc. Chem. Rev., 10* (1977) 265.

6 R. D. Jones, D. A. Summerville and F. Basolo, *Chem. Rev., 79* (1979) 139.

7 E. C. Niederhoffer, J. H. Timmons and A. E. Martell, *Chem. Rev., 84* (1984) 137.

8 B. R. James, A. W. Addison, M. Cairns, D. Dolphin, N. P. Farrell, D. R. Paulson and S. Walker, in M. Tsutsui (ed.), *Fundamental Research in Homogeneous Catalysis*, Vol. 3, Plenum, New York, 1979, pp. 751–772.

9 T. S. Srivastava, *Indian J. Chem. Soc. A, 20* (1981) 908.

10 D. R. Paulson, A. W. Addison, D. Dolphin and B. R. James, *J. Biol. Chem., 254* (1979) 7002.

11 I. Morishima, Y. Shiro and K. Nakajuma, *Biochemistry, 25* (1986) 3576.

12 (a) J. B. Kenneth, K. Andrew Jr. and R. S. Drago, *Inorg. Chem., 27* (1988) 2955; (b) K. D. Karlin, M. S. Haka, R. W. Cruse, G. J. Meyer, A. Farooq, Y. Gultneh, J. C. Heyes and J. Zubieta, *J. Am. Chem. Soc., 110* (1988) 1196.

13 W. P. Hart and M. D. Rausch, *J. Am. Chem. Soc., 102* (1980) 1196.

14 Y. Wakatsuki and H. Yamazaki, *Bull. Chem. Soc. Jpn., 58* (1985) 2715.

15 T. Sakurai and K. Kobayashi, *Rikagaku Kenkyusho Hokoku, 55* (1979) 69.

16 C. A. McAulliffe, R. V. Parish, F. M. Ashmaway, R. H. Issa and S. A. Amer, *J. Chem. Soc., Dalton Trans.*, (1986) 2009.

17 J. P. Collman, *Acc. Chem. Rev., 25* (1986) 4714.

18 J. E. Pate, R. W. Cruse, K. D. Carlin and E. I. Solomon, *J. Am. Chem. Soc., 109* (1987) 2624.

19 G. Cros and J. P. Laurent, *Inorg. Chim. Acta, 105* (1985) 63.

20 W. K. Wilmarth, S. Aranoff and M. Calvin, *J. Am. Chem. Soc., 68* (1946) 2263.

21 B. Bollote, D. J. Aymes and R. M. Paris, *Bull. Soc. Chim. Fr., 5/6* (1979) 141.

22 J. M. Ruder, *Evolution of Fluomine as an Oxygen Solvent, CSDTR-72*, 59 Air Force Systems Command, Wright Patterson Air Force Base Fairborn, OH, June 1972.

23 M. M. Taqui Khan, Ch. Sreelatha, S. A. Mirza, G. Ramachandraiah and S. H. R. Abdi, *Inorg. Chim. Acta, 154* (1988) 103.

24 J. P. Collman, J. I. Brauman, L. J. Brent, J. L. Sissler, R. M. Morris and Q. M. Gibson, *J. Am. Chem. Soc., 105* (1983) 3052.

25 T. G. Traylor, N. Koga and L. A. Deonduff, *J. Am. Chem. Soc., 107* (1985) 6504.

26 A. Szabo, *Proc. Natl. Acad. Sci. U.S.A., 75* (1978) 2108.

27 Y. Uemori and E. Kyuno, *Inorg. Chim. Acta, 9* (1987) 138.

28 M. M. Collman, R. K. Boggers, J. W. Hughes and L. T. Taylors, *Inorg. Chem., 20* (1981) 700.

29 M. M. Taqui Khan, S. A. Mirza, Z. A. Shaikh, Ch. Sreelatha, P. Paul, S. H. R. Abdi, S. D. Bhatt and G. Ramachandraiah, *Inorg. Chem.*, submitted for publication.

30 M. M. Taqui Khan, N. H. Khan, R. I. Kureshy, G. Ramachandraiah, S. A. Mirza and A. B. Boricha, *Inorg. Chim. Acta*, submitted for publication.

31 D. Chen and A. E. Martell, *Inorg. Chem., 26* (1987) 1026.

32 N. J. Rose and R. S. Drago, *J. Am. Chem. Soc., 81* (1959) 6138.

33 S. A. Patel and V. H. Kulkarni, *Polyhedron, 3* (1984) 21.

34 C. M. Che, K. Y. Wong and C. K. Poon, *Inorg. Chem., 24* (1985) 1797.

35 M. M. Taqui Khan, A. Hussain, G. Ramachandraiah and M. A. Moiz, *Inorg. Chem., 25* (1986) 3023.

36 M. M. Taqui Khan, Ch. Sreelatha, S. A. Mirza, G. Ramachandraiah and S. H. R. Abdi, *Inorg. Chim. Acta, 154* (1988) 103.

37 W. R. Harris, G. L. McLendon, A. E. Martell, R. C. Bess and M. Mason, *Inorg. Chem., 19* (1980) 1921.